

Article

Carboxylated Graphene Oxide (c-GO) Embedded ThermoPlastic Polyurethane (TPU) Mixed Matrix Membrane with Improved Physicochemical Characteristics

Muhammad Zahid ¹, Maryam Saeeda ¹, Nimra Nadeem ², Hafiz Muhammad Fayzan Shakir ³,
Waleed A. El-Saoud ⁴, Osama A. Attala ⁵, Kamal A. Attia ⁶ and Zulfiqar Ahmad Rehan ^{7,*}

¹ Department of Chemistry, University of Agriculture, Faisalabad 38040, Pakistan

² Department of Textile Engineering, School of Engineering and Technology, National Textile University, Faisalabad 37610, Pakistan

³ School of Materials Science and Engineering, Northwestern Polytechnical University, Xi'an 710060, China

⁴ Natural Hazards Research Unit, Department of Environmental and Health Research, Umm Al-Qura University, Mecca 21955, Saudi Arabia

⁵ Department of Environmental and Health Research, The Custodian of the Holy Mosques Institute for Hajj and Umrah Research, Umm Al-Qura University, Mecca 21955, Saudi Arabia

⁶ Biology Department, Al-Jammoum University College, Umm Al-Qura University, Makkah 24381, Saudi Arabia

⁷ Department of Materials, National Textile University, Faisalabad 37610, Pakistan

* Correspondence: zarehan@ntu.edu.pk

Abstract: Water is an important component of our life. However, the unavailability of fresh water and its contamination are emerging problems. The textile industries are the major suppliers of contamination of water, producing high concentrations of heavy metals and hazardous dyes posing serious health hazards. Several technologies for water purification are available in the market. Among them, the membrane technology is a highly advantageous and facile strategy to remediate wastewater. Herein, the distinguished combination of pore-forming agents, solvent, and nanoparticles has been used to achieve improved functioning of the polymeric composite membranes. To do so, graphene oxide (GO) was fabricated via Hummer's technique and GO functionalization using chloroacetic acid (c-GO) was performed. Thermoplastic polyurethane (TPU) membranes having different concentrations c-GO were made using the phase inversion technique. Scanning electron microscopy (SEM), Fourier transforms infrared spectroscopy (FT-IR), and X-ray diffraction (XRD) was used to examine surface morphology, chemical functionalities on membranes surfaces, and crystallinity of membranes, respectively. The temperature-dependent behavior of c-GO composite membranes has been analyzed using DSC technique. The water contact angle measurements were performed for the estimation of hydrophilicity of the c-GO based TPU membrane. The improved water permeability of the composite membrane was observed with increasing the c-GO concentration in polymeric membranes. c-GO was observed as a potential candidate that enhanced membrane physicochemical properties. The proposed membranes can behave as efficient candidates in multiple domains of environmental remediation. Furthermore, the improved dye rejection characteristics of proposed composite membranes suggest that the membranes can be best suited for wastewater treatment as well.

Keywords: thermoplastic polyurethane (TPU); carboxylated graphene oxide (c-GO); nanocomposite membrane; water flux; dye rejection



Citation: Zahid, M.; Saeeda, M.; Nadeem, N.; Shakir, H.M.F.; El-Saoud, W.A.; Attala, O.A.; Attia, K.A.; Rehan, Z.A. Carboxylated Graphene Oxide (c-GO) Embedded ThermoPlastic Polyurethane (TPU) Mixed Matrix Membrane with Improved Physicochemical Characteristics. *Membranes* **2023**, *13*, 144. <https://doi.org/10.3390/membranes13020144>

Academic Editor: Tan Yong Zen

Received: 16 December 2022

Revised: 14 January 2023

Accepted: 19 January 2023

Published: 22 January 2023



Copyright: © 2023 by the authors. Licensee MDPI, Basel, Switzerland. This article is an open access article distributed under the terms and conditions of the Creative Commons Attribution (CC BY) license (<https://creativecommons.org/licenses/by/4.0/>).

1. Introduction

Pure water is essential and a major component for human survival on this planet [1]. Drinking water, both in terms of quality and quantity, has become a critical challenge for human survival [2]. The expansion of industries, agricultural resources, and the population

growth all demands access to clear water [3]. The textile industries are the major contributor of colored wastewater production [4,5]. It is the biggest zone that is spreading extreme water pollution. Chemical additives and various types of dyes are also present in textile wastewater. The problem of colors in textile effluent and the difficulties related to the degradation of dye wastewater is alarming [6–10]. There is a need to design solutions that are cost effective and time efficient to recover and provide high quality of water.

Membrane technology is used in a number of water treatment processes for this purpose, including municipal and industrial wastewater recycling, and also sea- and brackish water desalination [11,12]. A membrane is a thin sheet or layer that serves as a selective barrier between two phases (liquid, vapor, or gas), allowing certain components to flow through depending on its structure [13,14]. Membranes are advantageous because of their low production cost, energy efficiency, ease of fabrication, and lack of thermal treatment [15]. Polymeric membranes have drawn a lot of interest due to their high-water flux, environmental friendliness, cost-effectiveness, and energy efficiency. Polymer-based membranes are composed up of polymers and organic matter including polyether sulfone, polysulfone, polyether ketone, thermoplastic polyurethane (TPU), cellulose acetate (CA), polyimide (PI), polysulfide (PS) (Espinoza et al., 2014) for treatment of wastewater. Most polymeric membranes are either hydrophobic or have low hydrophilicity. TPU (thermoplastic polyurethane) is an engineered thermoplastic polymer with good mechanical characteristics. TPU network structure is made up of soft and rigid segments, giving it qualities resembling rubbery and unstructured thermoplastics. To improve the features of TPU such as hydrophilic nature, smooth surface, the charge on the surface, and antibacterial activity, selective advancement in the membrane could be carried out to increase water permeability (Riaz et al., 2016). Functionalized nanoparticles and pore-forming agents are gaining attention of scientific community to improve the physicochemical characteristics of TPU. Due to its excellent mechanical characteristics, high surface area, ease of creation of dense membrane structures, and superior water dispersal ability graphene oxide (GO) have emerged as a potential membrane nanomaterial [16]. Multiple oxygen functional groups in GO such as COOH, epoxy, carbonyl, and -OH, improve its hydrophilicity and provide remarkable characteristics [17–23]. Functionalized carboxylated graphene oxide-based membranes may be used to remove ionic dyes [24], and changing hydroxyl groups and ether linkages into carboxyl groups might increase the membrane's performance.

Here we proposed the fabrication of novel carboxylated graphene oxide polyurethane membrane (c-GO/TPU) by NIPS method. Different concentrations of c-GO were selected to form TPU based composite membranes. All the membranes were well characterized in term of surface morphology using SEM, surface functional groups using FTIR, and membranes crystallinity using XRD analysis. Moreover, the mechanical strength of pristine TPU and c-GO embedded TPU membranes were checked using tensile strength estimation approach. The pure water flux potential and dye rejection efficiency of membranes were also analyzed. The effect of c-GO content addition on the hydrophilicity of membranes was analyzed using water contact angle measurements. The DSC approach was accessed to analyze the thermal characteristics of selected membranes. The extensive analysis of c-GO based TPU composite membranes suggest that the addition of c-GO content improves the surface morphology, hydrophilicity, and mechanical strength characteristics. Therefore, depending upon the application area, the proposed membranes can be an efficient candidate in multiple domains of environmental remediation. Furthermore, the improved dye rejection characteristics of proposed composite membranes suggest that the membranes can be best suited for wastewater treatment as well.

2. Materials and Methods

2.1. Materials

Thermoplastic polyurethane was obtained from Townsend Corporation (RE-FLEX585-XU, MW = 25KD). Graphite powder (average particle size of <20 μm), and phosphoric acid (H_3PO_4) were bought from Sigma-Aldrich. Potassium permanganate (KMnO_4 Mw

~158.03, Assay = 99.5%) was purchased from AnalAR[®]. Sodium hydroxide pellets (NaOH: 98% Analytic-ACS) were purchased from ICON CHEMICAL. Polyvinyl pyrrolidone (PVP of Mw ~40,000 Da), sulfuric acid (H₂SO₄ Assay 98.5%), Hydrogen peroxide (H₂O₂; 30%) aqueous solution, and N, N-Dimethyl formamide (DMF) were purchased from DAEJUNG. Chloroacetic acid (C₂H₃ClO₂: 94.49 g/mol⁻¹) was purchased from Merck, Germany. Deionized water (DI) used in this study was produced through an integrated system of a Milli-Q (Merck Millipore, Ireland). All compounds were of analytical rank and were used exactly as directed.

2.2. Synthesis

2.2.1. Preparation of Graphene Oxide

Graphene oxide was fabricated using modified Hummer's method. The detailed process is described somewhere else [25].

2.2.2. Synthesis of Carboxylated Graphene Oxide (c-GO)

Carboxylated graphene oxide was synthesis by the reaction of chloroacetic acid with sodium hydroxide. For this 0.5 g of graphene oxide was added into 250 mL distilled water and sonicated for 1 h to form suspension. After complete dispersion, 3.6 g of sodium hydroxide was added, and solution was again sonicated for 1 h. Then, the 10 g of chloroacetic acid was added into the reaction mixture and ultra-sonicated for 1 h. The obtained c-GO was washed several times with DI water until the pH of the solution becomes neutral. The c-GO was then dried in the oven overnight at 70 °C.

2.2.3. Fabrication of Carboxylated Graphene Oxide Based TPU Membranes

Carboxylated graphene oxide TPU based membranes were fabricated by phase inversion method. In the first step, c-GO was sonicated in DMF for 1 h 15 percent TPU was dissolved in DMF to make the membrane casting solution. Under magnetic stirring, different quantities of c-GO (Table 1.) with fixed number of pore-forming agents (PVP) was introduced to the TPU solution for full dissolution. The solution was then allowed to stir for 4 to 6 h to remove air bubbles and to make it homogeneous. The obtained solution was cast on a 500 μm thick film applicator. The casted membrane was immersed into the distilled water bath for solvent exchange. After two minutes, the c-GO embedded TPU membrane was detached from the casting plate. The membrane was dried at room temperature. All the membranes with different concentrations of carboxylated graphene were fabricated using similar approach. The schematic representation of membrane casting process is presented in Figure 1.

Table 1. Compositions of c-GO based TPU membranes.

Membrane	TPU (wt %)	PVP	DMF	c-GO
TPU	15%	0%	85%	-
c-GO 0	15%	0%	84.9%	0.1%
c-GO 1	15%	5%	79.8%	0.2%
c-GO 2	15%	5%	79.7%	0.3%
c-GO 3	15%	5%	79.6%	0.4%
c-GO 4	15%	5%	79.5%	0.5%

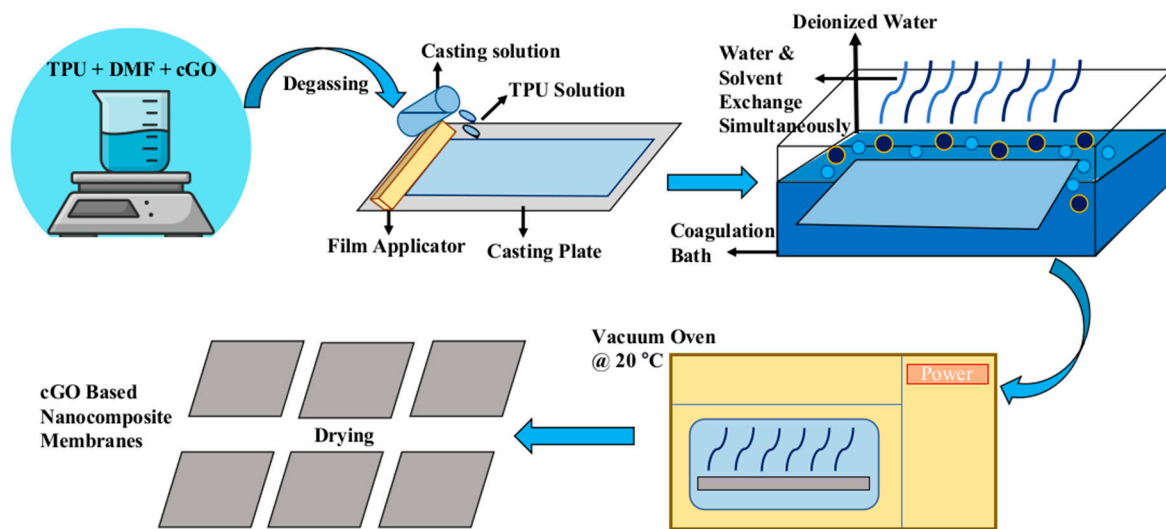


Figure 1. Schematic representation of phase inversion method.

2.3. Characterization of GO and c-GO and TPU Composite Membranes

Characterization of fabricated composite membrane was carried out by different techniques such as FE-SEM, XRD, FTIR spectroscopy, contact angle and tensile strength. Field emission scanning electron microscopy was used to examine the surface morphology of membranes (FEI, Quanta FEG 450). Membrane samples were copper taped to the grid and sputtered with gold using a sputter coater (Quorum Q150R ES, Quorum Technologies Ltd., Ashford, Kent, England). The presence of functional groups at different blend and solution formulations was identified using FTIR spectroscopy (FTIR; Bruker Tensor 27, Billerica, MA, USA). XRD analysis was used to examine the micro sheet samples (Bruker-AXS diffractometer, Karlsruhe, Germany). A goniometer OCA15EC was used to measure the contact angle of water on membrane surfaces using the sessile drop method at ambient temperature (Dataphysics, Karlsruhe, Germany). Thermal analysis was conducted at a 10 °C/min heating rate under nitrogen atmosphere using DSC technique.

2.4. Measurement of Water Contact Angle, Pure Water Flux and Dye Rejection Rate

The contact angle was measured using a contact angle measuring device and the sessile-drop technique. A droplet of water was placed on the membrane surface and the contact angle of the droplet with the surface was computed using this approach. The contact angle was measured at five random points on each membrane to minimize the research error, and the average of results is reported. A cross-filtration equipment was used to assess the membrane's pure water flow.

Hydrophilic properties of all fabricated membranes were examined by Attension Theta Tensiometer using measurement of water contact angle. To do so, water was utilized by means of probe liquid. The fixed contact angle (made between the drop of water and the surface of membrane) was determined at room temperature via the sessile drop mode using goniometer device. The contact angle was calculated by averaging five measurements performed at various points across the surface of membrane [11,18].

The tensile strength of the c-GO based membranes were measure using Instron tensile test equipment. Membranes were cut into a standard form prior to testing. The thermal characteristics of c-GO/TPU membranes were determined using differential scanning calorimeter (DSC 250 from TA, New Castle, USA) instrument. Prepared membranes weighing 10 mg were encapsulated in an aluminum pan and tested at temperatures ranging from 25 to 300 degrees Celsius at a rate of 10 degrees Celsius per minute under a N₂ environment [11].

A lab-scale cartridge filter was used at cross-end mode operation to examine the permeate flux of water as well as rejection of dye by c-GO/TPU membranes. Pressure

gauges are the major constituents of the filtration system, a 2-L feed tank (having mixer and temperature control), low as well as high pressure feed pumps (1–15 bar), and stainless-steel flat membrane module (effective area of 8.6 cm²) were equipped with the reaction system. Before measurements of flux, membranes remained soaked in distilled water for 24 h. The membranes were then compacted for 30 min at less than 2 bar of distilled water until a steady flow was attained. The pressure instantly decreased to 1 bar, and a pure water flux test was carried out for 1 h. The volume of filtrate was collected and measured after every 5 min. In conclusion, the Equation (1) was used to compute the flow [26].

$$J = \frac{V}{A\Delta T} \quad (1)$$

where V stands for the permeated volume of pure water (L), A is the operative membrane area (m²), ΔT stands for the sampling time (h) and J_w is the pure water flux (L/m² h).

The dye rejection potential of all membranes was analyzed using aqueous solution of Coomassie Blue dye. The feed solution was prepared by 0.01 g/cm³ Coomassie Blue in ethanol. This solution was used as feed solution to make 2 L of aqueous solution with the dye concentration of 10 ppm at neutral pH (25 °C). The formula given Equation (2) below was used to calculate dye rejection [27].

$$R = \left(1 - \frac{C_p}{C_f}\right) \times 100 \quad (2)$$

In above equation R is membrane rejection, C_f is dye concentration in the feed and C_p is dye concentration at permeate side.

2.5. Membrane Porosity Determination Using Gravimetric Method

Gravimetric method was used to determine the membrane porosity. To do so, all membranes were oven dried and weighed before experiment. The membranes were then immersed in kerosene oil for 24 h and reweighed. The average porosity was determined in terms of overall void fraction which can be calculated as the pore volume divided by the total membrane volume. The average porosity was calculated using the formula given in Equation (3):

$$\varepsilon_m \% = \left[\frac{W_1 - W_2}{D_k} \right] / \left[\frac{W_1 - W_2}{D_k} + \frac{W_2}{D_{pol}} \right] \times 100 \quad (3)$$

where

$$W_1 = \text{weight of wet membrane}, W_2 = \text{weight of dry membrane}, \\ D_k = \text{density of kerosene oil} \left(0.82 \frac{\text{g}}{\text{cm}^3}\right), D_{pol} = \text{density of polymer}$$

3. Result and Discussion

3.1. Characterization of Nanoparticles

The FTIR spectral information is presented in Figure 2. Figure 2 presents the FTIR spectra of GO and c-GO. The stretching vibrations of the hydroxyl (O-H) groups upon graphene oxide are represented by a broad peak in the upper-frequency band of 3445 cm⁻¹ [28,29]. The absorption peaks at 2850 cm⁻¹ show the stretching vibration of CH₂. The ketone group is responsible for the appearance of a peak at 1627 cm⁻¹, and sp² hybridization is responsible for the primary graphitic domain of the peak at 1544 cm⁻¹. The C-O is shown by the band at 1457 cm⁻¹, whereas the C-O stretching of epoxy groups is indicated by the band at 1243 cm⁻¹. The C-O-C stretching of alkoxy groups is revealed by the mode at 1087 cm⁻¹. Compared to spectra of GO and c-GO, the vibration band of C-O-C has observed on the 1052 cm⁻¹ and OH shows absorption peak on the 1349 cm⁻¹. The absorption peak of C=O was around 1620 cm⁻¹ become broader and high strength. This peak was overlapped the -COOH peak at 1720 cm⁻¹. Between 3000 and 3500 cm⁻¹, a hydroxyl group (-OH) adsorption band was identified, indicating a substantial quantity of carboxyl group on

the graphene surface. the results also support clear evidence about successful formation of c-GO as the peaks corresponding to carboxylic groups i.e., peaks at 1728 cm^{-1} and 1614 cm^{-1} showed clear enhancement in C-GO. Similarly, the peak ascribed to aromatic group also showed clear enhancement in c-GO [30].

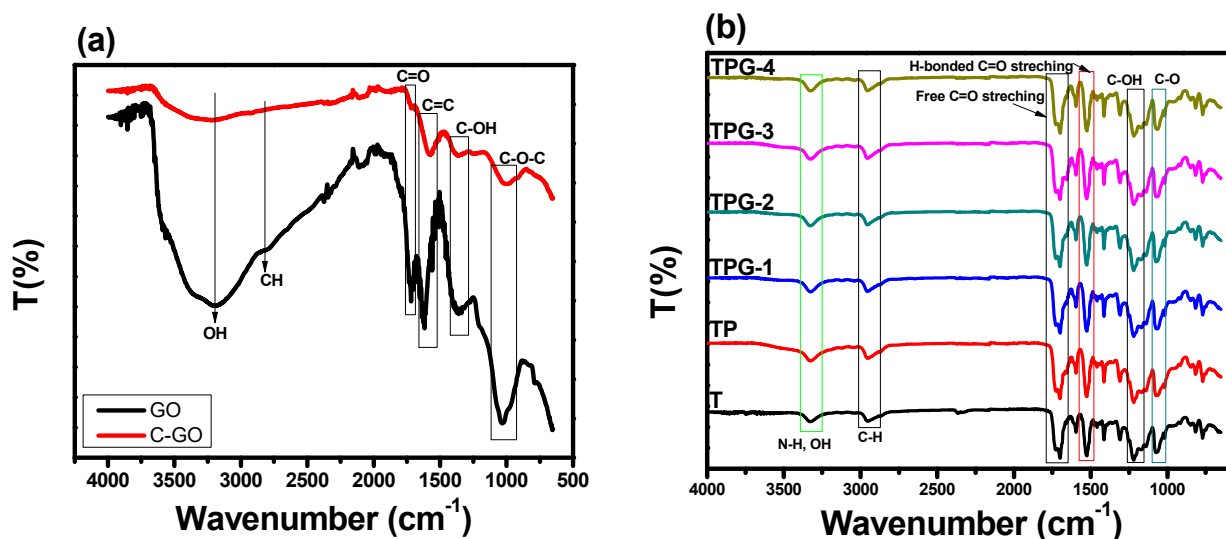


Figure 2. FTIR spectra of (a) GO and c-GO, (b) pristine TPU and c-GO embedded TPU membranes.

Figure 2b represents the FTIR spectra of thermoplastic polyurethane membrane, PVP-based TPU membranes, and TPU membrane with different concentrations of carboxylated graphene oxide. The FTIR spectra of TPU exhibit a transmittance peak at 3330 cm^{-1} corresponds to the -NH group. The peak positioned at 2960 cm^{-1} is ascribed to the CH_2 . Another peak at 1215 cm^{-1} is representative of the C-N-H bonding. The functional groups of C-O-C in TPU exhibits peak at 1120 cm^{-1} . The spectrum of TPU-PVP shows absorption bands at 1639 cm^{-1} and 1215 cm^{-1} which denote carbonyl and amide groups. Carboxylated graphene oxide-based TPU membranes exhibit peaks at 3330 cm^{-1} , 2960 cm^{-1} , 1687 cm^{-1} , 1516 cm^{-1} , 1215 cm^{-1} , and 1120 cm^{-1} . All these peaks are present in the carboxylated graphene oxide ensuring successful insertion of c-GO into thermoplastic polyurethane membranes matrix.

3.1.1. SEM Analysis

SEM investigation confirms the surface morphology of TPU and TPU composite membranes, as shown in Figure 3. The SEM pictures of TPU composite membranes with varying quantities of c-GO content demonstrate the presence of particles on the membrane's surface. Water addition during casting solution preparation may have generated a rough picture that correlates to fractures and ridges in c-GO 4 (0.5 wt percent). Particle aggregates appear on the surface of the c-GO 4 membrane at intervals, indicating particle dispersion inside the polymeric substance. The insertion of c-GO in pristine TPU (Figure 3a) results extraordinary improvement in morphology of composite membranes. The improved morphology is attributed to the increased surface roughness owing to the nano-dimensional c-GO loading. High surface roughness is effective in generating surface defects which contribute towards improved adsorption properties of membranes as well.

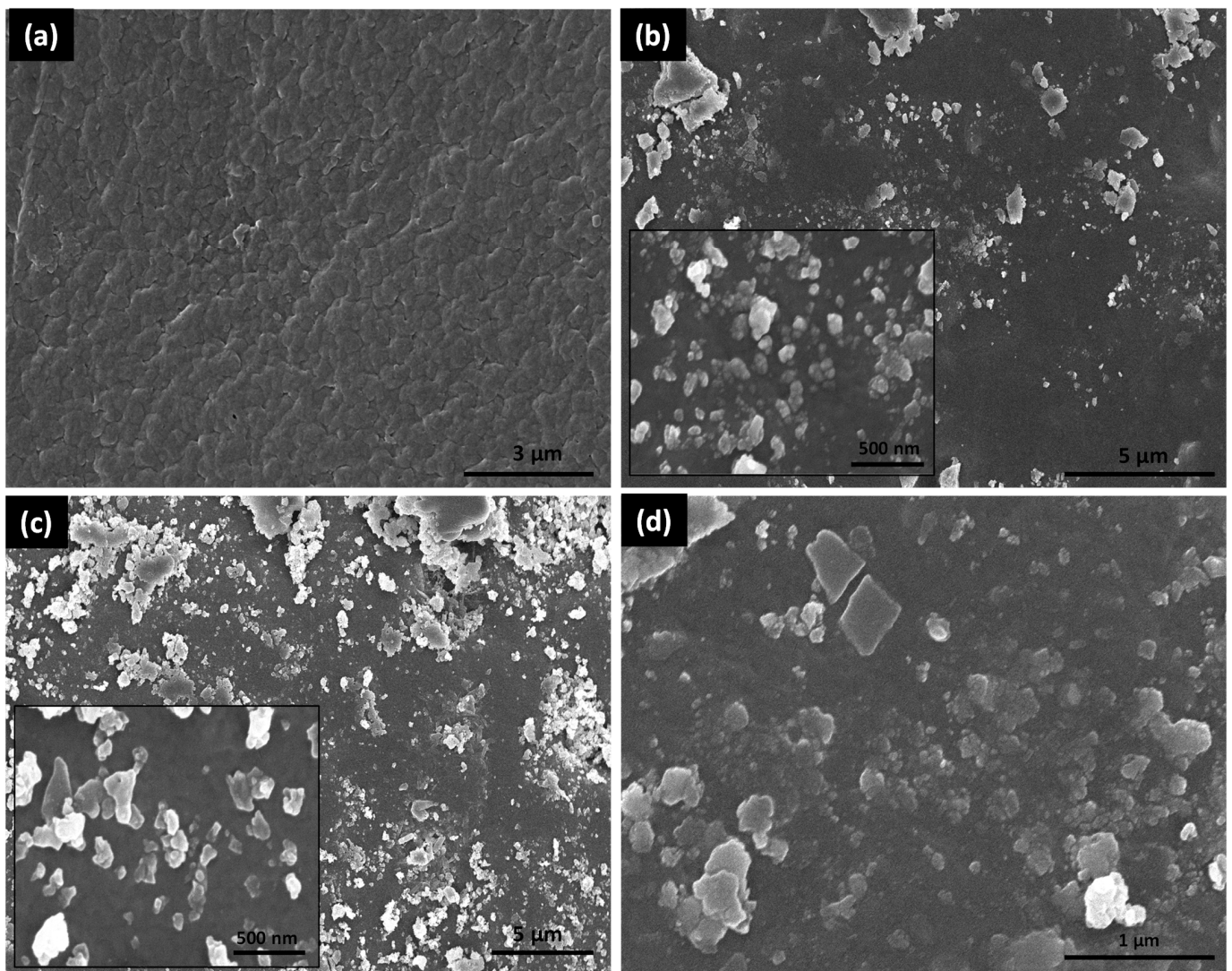


Figure 3. SEM images of (a) TPU (b) c-GO 1, (c) c-GO 3, and (d) c-GO 4.

3.1.2. XRD

Figure 4 presents the XRD analysis of all c-GO based TPU membranes. A broad peak in the range of 11° – 20° is ascribed to the amorphous nature of TPU. Insertion of c-GO into the matrix of TPU does not significantly change the peak structure. However, peak broadening supports the incorporation of c-GO. C-GO exhibits characteristic peak around $2\theta = 10^{\circ}$ [31], no clear indication of peaks located at $2\theta = 10^{\circ}$ in composite membrane suggests that c-GO was well incorporated with TPU matrix [32].

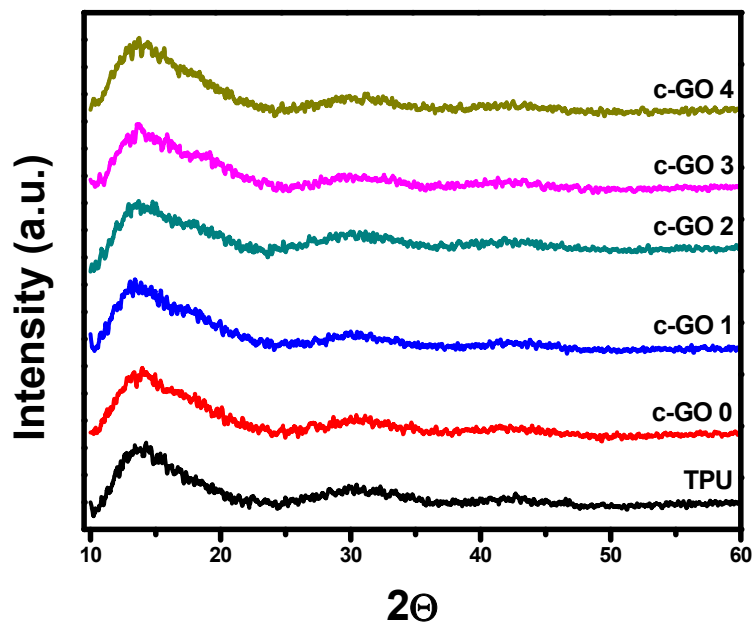


Figure 4. XRD pattern of TPU, and c-GO based TPU membranes.

3.1.3. Contact Angle

Membrane contact angle measurements are commonly used to determine membrane surface hydrophilicity. Figure 5 presents that the contact angle of pristine TPU membrane is 76.95 decreased with the addition of different concentrations of carboxylated graphene oxide into membranes to 68.86, 61.01, 57.97, and 54.00 for c-GO 1, c-GO 2, c-GO 3, and c-GO 4, respectively. This suggested that the surface hydrophilicity has improved as a result of the addition of c-GO micro sheets, as previously observed [33] and corroborated by the pure water flow. A huge number of the micro sheets' -COOH groups orient themselves towards the water, inducing hydrophilic characteristics on the membrane, which promotes water adsorption and hence improves water permeability [34].

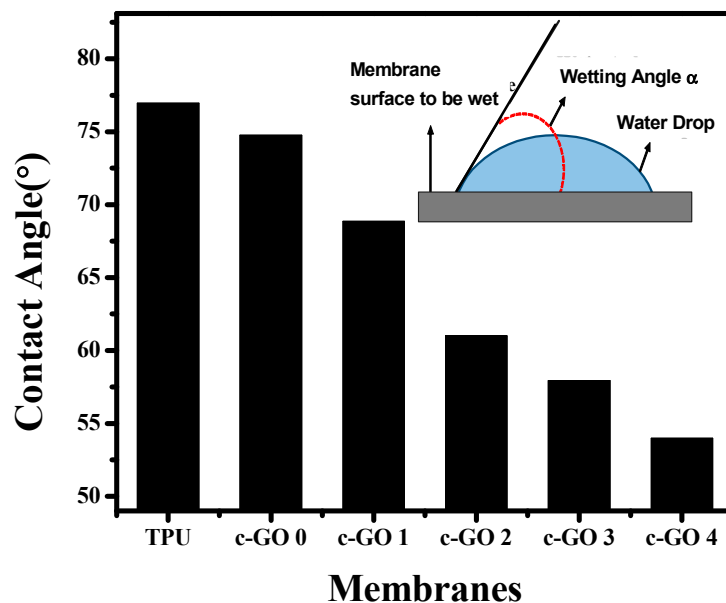


Figure 5. The contact angle of TPU and composite membranes.

3.1.4. DSC

DSC curves of prepared TPU/c-GO membranes with different concentrations in this study are given in Figure 6. The T_g (Glass transition temperature) is generally used for interpretation of membrane structure while employing the thermal analysis upon membrane. The glass transition temperature of the pristine TPU is greater than the TPU/c-GO composite membranes (i.e., c-GO 0 and c-GO 4). With the addition of the carboxylated graphene oxide T_g of TPU decreased slightly i.e., 204 °C for pristine TPU to 202 °C and 201 °C for c-GO 0 and c-GO 4, respectively. Aside from c-GO, the reduction may be attributed to PVP's plasticization effect since PVP can be used as a stabilizer and plasticizer for polymers [35]. The slight thermal degradation of c-GO 0 and c-GO 4 could be due to the interactions of c-GO and PVP with TPU network and good thermal conductivity of c-GO resulting in creation of degradation centers in composite membranes.

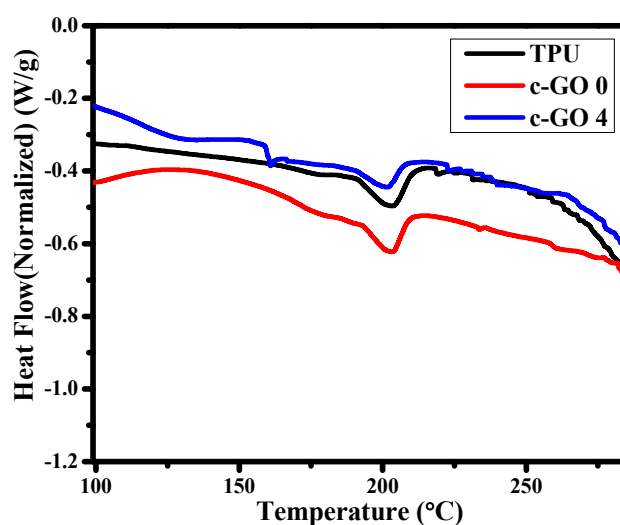


Figure 6. DSC thermogram of pristine TPU and TPU based composite membranes (c-GO 0 and c-GO4).

3.1.5. Pure Water Flux of Membranes

One of the most important characteristics to consider when evaluating the performance of a manufactured membrane is its permeability to pure water. Figure 7 showed that with the addition of c-GO to the membrane matrix, the penetration fluxes of the membranes were improved. The water flux of the pure TPU membrane was 21.81 LMH and c-GO 4 was 142 LMH. Due to the addition of c-GO to membrane, porosity increase that causes high water flux. The oxygen-rich functional groups of the c-GO that have migrated to the top surface of the membranes have also increased the membranes' hydrophilicity. Furthermore, c-GO nanofillers demonstrated a reduction in contact angle, which might help to improve water permeability [36]. Furthermore, the results of membrane porosity support the conclusion that increased membrane porosity by increasing c-GO content helps improve water flux (Table 2).

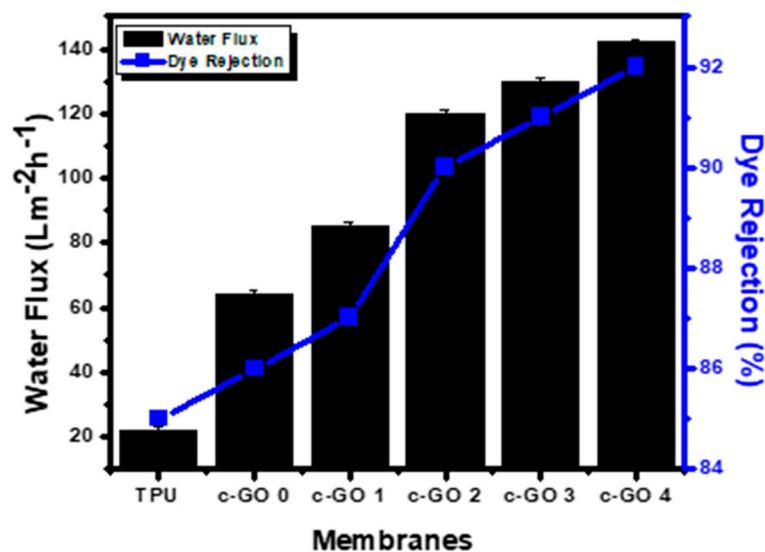


Figure 7. Pure water flux and dye rejection performance of TPU and c-GO/TPU membranes (Dye Coomassie Blue (10 ppm), pH = 7, T = 30 °C).

Table 2. Porosity (%) of TPU based c-GO composite membranes.

Sr#	Membranes	Porosity (%)
1	TPU	72.48
2	c-GO 0	74.70
3	c-GO 1	87.54
4	c-GO 2	88.53
5	c-GO 3	90.42
6	c-GO 4	91.26

3.1.6. Dye Rejection by Composite Membrane

Due to its excellent removal performance, and low operating cost, many types of membrane technology have been used to remove synthetic colours from wastewater. The dye rejection rate of the membrane rises when nanoparticles are added to it (due to improved morphology). Therefore, the dye rejection experiment was performed and results are presented in Figure 7. Increasing the c-GO content in TPU matrix improved the surface morphology in term of surface defect thereby improving the adsorption capability of composite membranes which results in high dye rejection [37].

The results of membranes porosity calculated by gravimetric analysis is presented in Table 2. A rapid increase in membrane porosity was observed when pristine TPU membranes were composited with c-GO. The membrane porosity of pristine TPU was observed as 72.48% which increases to 87.54% with the addition of c-GO (1 wt %). Increased water flux can be correlated with the improved structure in term of membrane porosity. Among c-GO based TPU membranes an increasing trend of membrane porosity was observed by increasing c-GO content which also support the porosity induction is due to c-GO insertion.

4. Conclusions

In conclusion, the phase inversion method was used to produce TPU membranes containing variable c-GO content. All the membranes were well characterized in term of SEM, FTIR, and XRD analysis. Moreover, the mechanical strength of pristine TPU and c-GO embedded TPU membranes were checked using tensile strength estimation approach. The pure water flux potential and dye rejection efficiency of membranes were also analyzed. The effect of c-GO content addition on the hydrophilicity of membranes was analyzed using

water contact angle measurements. With the addition of c-GO nanoparticles to the TPU polymer matrix, water absorption was increased while the contact angle was reduced. c-GO-4 had the highest water flow while having a lowest contact angle among all membranes. The DSC approach was accessed to analyze the thermal characteristics of selected membranes and little reduction in T_g was observed when TPU was composited with c-GO (owing to the degradation centers generation due to good thermal conductivity of c-GO). The extensive analysis of c-GO based TPU composite membranes suggest that the addition of c-GO content improves the surface morphology, hydrophilicity, and mechanical strength characteristics. Therefore, depending upon the application area, the proposed membranes can behave as efficient candidate in multiple domains of environmental remediation. Moreover, the improved dye rejection characteristics of proposed composite membranes suggest that the membranes can be best suited for wastewater treatment as well.

Author Contributions: Conceptualization, M.Z.; methodology, M.Z. and Z.A.R.; Software, H.M.F.S. and K.A.A.; Validation, K.A.A.; Formal analysis, N.N.; Investigation, M.Z. and H.M.F.S.; Resources, W.A.E.-S. and O.A.A.; Data curation, M.S. and N.N.; Writing – original draft, M.Z. and M.S.; Writing – review & editing, K.A.A. and Z.A.R.; Visualization, W.A.E.-S.; Supervision, Z.A.R.; Project administration, Z.A.R.; Funding acquisition, O.A.A. All authors have read and agreed to the published version of the manuscript.

Funding: The authors would like to thank the Deanship of Scientific Research at Umm Al-Qura University for supporting this work by Grant Code: 22UQU4350532DSR02.

Institutional Review Board Statement: Not applicable.

Informed Consent Statement: Not applicable.

Data Availability Statement: Not applicable.

Conflicts of Interest: The Authors declare no conflict of interest.

References

1. Qamar, M.; Aslam, M.; Rehan, Z.; Soomro, M.; Basahi, J.M.; Ismail, I.M.; Hameed, A. The effect of Fe³⁺ based visible light receptive interfacial phases on the photocatalytic activity of ZnO for the removal of 2, 4-dichlorophenoxy acetic acid in natural sunlight exposure. *Sep. Purif. Technol.* **2017**, *172*, 512–528. [\[CrossRef\]](#)
2. Ghaee, A.; Zerafat, M.; Askari, P.; Sabbaghi, S.; Sadatnia, B. Fabrication of polyamide thin-film nanocomposite membranes with enhanced surface charge for nitrate ion removal from water resources. *Environ. Technol.* **2017**, *38*, 772–781. [\[CrossRef\]](#)
3. Yin, J.; Deng, B. Polymer-matrix nanocomposite membranes for water treatment. *J. Membr. Sci.* **2015**, *479*, 256–275. [\[CrossRef\]](#)
4. Cinperi, N.C.; Ozturk, E.; Yigit, N.O.; Kitis, M. Treatment of woolen textile wastewater using membrane bioreactor, nanofiltration and reverse osmosis for reuse in production processes. *J. Clean. Prod.* **2019**, *223*, 837–848. [\[CrossRef\]](#)
5. Yaseen, D.A.; Scholz, M. Textile dye wastewater characteristics and constituents of synthetic effluents: A critical review. *Int. J. Environ. Sci. Technol.* **2018**, *16*, 1193–1226. [\[CrossRef\]](#)
6. Chen, X.; Shen, Z.; Zhu, X.; Fan, Y.; Wang, W. Advanced treatment of textile wastewater for reuse using electrochemical oxidation and membrane filtration. *Water Sa* **2005**, *31*, 127–132. [\[CrossRef\]](#)
7. Nadeem, N.; Zahid, M.; Rehan, Z.A.; Hanif, M.A.; Yaseen, M. Improved photocatalytic degradation of dye using coal fly ash-based zinc ferrite (CFA/ZnFe₂O₄) composite. *Int. J. Environ. Sci. Technol.* **2022**, *19*, 3045–3060. [\[CrossRef\]](#)
8. Ashiq, H.; Nadeem, N.; Mansha, A.; Iqbal, J.; Yaseen, M.; Zahid, M.; Shahid, I. G-C₃N₄/Ag@CoWO₄: A novel sunlight active ternary nanocomposite for potential photocatalytic degradation of rhodamine B dye. *J. Phys. Chem. Solids* **2021**, *161*, 110437. [\[CrossRef\]](#)
9. Nadeem, N.; Abbas, Q.; Yaseen, M.; Jilani, A.; Zahid, M.; Iqbal, J.; Murtaza, A.; Janczarek, M.; Jesionowski, T. Coal fly ash-based copper ferrite nanocomposites as potential heterogeneous photocatalysts for wastewater remediation. *Appl. Surf. Sci.* **2021**, *565*, 150542. [\[CrossRef\]](#)
10. Nadeem, N.; Zahid, M.; Hanif, M.A.; Bhatti, I.A.; Shahid, I.; Rehan, Z.A.; Hussain, T.; Abbas, Q. Silver-doped metal ferrites for wastewater treatment. In *Silver Nanomaterials for Agri-Food Applications*; Elsevier: Amsterdam, The Netherlands, 2021; pp. 599–622.
11. Senusi, F.; Shahadat, M.; Ismail, S.; Abd Hamid, S. Recent advancement in membrane technology for water purification. In *Modern Age Environmental Problems and their Remediation*; Springer: Cham, Switzerland, 2018; pp. 147–167.
12. Zahid, M.; Akram, S.; Rashid, A.; Rehan, Z.A.; Javed, T.; Shabbir, R.; Hessien, M.M.; El-Sayed, M.E. Investigating the antibacterial activity of polymeric membranes fabricated with aminated graphene oxide. *Membranes* **2021**, *11*, 510. [\[CrossRef\]](#)
13. Khajouei, M.; Peyravi, M.; Jahanshahi, M. The potential of nanoparticles for upgrading thin film nanocomposite membranes—A review. *J. Membr. Sci. Res.* **2017**, *3*, 2–12.

14. Ali, A.; Tufa, R.A.; Macedonio, F.; Curcio, E.; Drioli, E. Membrane technology in renewable-energy-driven desalination. *Renew. Sustain. Energy Rev.* **2018**, *81*, 1–21. [[CrossRef](#)]
15. Ng, L.Y.; Mohammad, A.W.; Leo, C.P.; Hilal, N. Polymeric membranes incorporated with metal/metal oxide nanoparticles: A comprehensive review. *Desalination* **2013**, *308*, 15–33. [[CrossRef](#)]
16. Fathizadeh, M.; Xu, W.L.; Zhou, F.; Yoon, Y.; Yu, M. Graphene oxide: A novel 2-dimensional material in membrane separation for water purification. *Adv. Mater. Interfaces* **2017**, *4*, 1600918. [[CrossRef](#)]
17. Dreyer, D.R.; Park, S.; Bielawski, C.W.; Ruoff, R.S. The chemistry of graphene oxide. *Chem. Soc. Rev.* **2010**, *39*, 228–240. [[CrossRef](#)]
18. Chen, J.; Peng, H.; Wang, X.; Shao, F.; Yuan, Z.; Han, H. Graphene oxide exhibits broad-spectrum antimicrobial activity against bacterial phytopathogens and fungal conidia by intertwining and membrane perturbation. *Nanoscale* **2014**, *6*, 1879–1889. [[CrossRef](#)] [[PubMed](#)]
19. Nisa, M.-U.; Nadeem, N.; Yaseen, M.; Iqbal, J.; Zahid, M.; Abbas, Q.; Mustafa, G.; Shahid, I. Applications of graphene-based tungsten oxide nanocomposites: A review. *J. Nanostruct. Chem.* **2022**. [[CrossRef](#)]
20. Tabasum, A.; Alghuthaymi, M.; Qazi, U.Y.; Shahid, I.; Abbas, Q.; Javaid, R.; Nadeem, N.; Zahid, M. UV-Accelerated Photocatalytic Degradation of Pesticide over Magnetite and Cobalt Ferrite Decorated Graphene Oxide Composite. *Plants* **2021**, *10*, 6. [[CrossRef](#)]
21. Tabasum, A.; Bhatti, I.A.; Nadeem, N.; Zahid, M.; Rehan, Z.A.; Hussain, T.; Jilani, A. Degradation of acetamiprid using graphene-oxide-based metal (Mn and Ni) ferrites as Fenton-like photocatalysts. *Water Sci. Technol.* **2020**, *81*, 178–189. [[CrossRef](#)]
22. Zahid, M.; Nadeem, N.; Hanif, M.A.; Bhatti, I.A.; Bhatti, H.N.; Mustafa, G. Metal ferrites and their graphene-based nanocomposites: Synthesis, characterization, and applications in wastewater treatment. In *Magnetic Nanostructures*; Springer: Cham, Switzerland, 2019; pp. 181–212.
23. Zahid, M.; Nadeem, N.; Tahir, N.; Majeed, M.I.; Naqvi, S.A.R.; Hussain, T. Hybrid nanomaterials for water purification. In *Multifunctional Hybrid Nanomaterials for Sustainable Agri-Food and Ecosystems*; Elsevier: Amsterdam, The Netherlands, 2020; pp. 155–188.
24. Lv, S.; Wei, J.; Jiang, F.; Wang, S. Adsorption-decolorization of four ionic dyes by carboxylated graphene. *Chin. J. Appl. Chem.* **2013**, *30*, 1215. [[CrossRef](#)]
25. Zubair, U.; Zahid, M.; Nadeem, N.; Ghazal, K.; AlSalem, H.S.; Binkadem, M.S.; Al-Goul, S.T.; Rehan, Z.A. The Design of Ternary Composite Polyurethane Membranes with an Enhanced Photocatalytic Degradation Potential for the Removal of Anionic Dyes. *Membranes* **2022**, *12*, 630. [[CrossRef](#)] [[PubMed](#)]
26. Li, J.; Liu, D.; Li, B.; Wang, J.; Han, S.; Liu, L.; Wei, H. A bio-inspired nacre-like layered hybrid structure of calcium carbonate under the control of carboxyl graphene. *CrystEngComm* **2015**, *17*, 520–525. [[CrossRef](#)]
27. Alfalahy, H.N.; Al-Jubouri, S.M. Preparation and application of polyethersulfone ultrafiltration membrane incorporating NaX zeolite for lead ions removal from aqueous solutions. *Desalin. Water Treat* **2022**, *3*, 28–56. [[CrossRef](#)]
28. Abdullah, M.; Al-Jubouri, S. Implementation of hierarchically porous zeolite-polymer membrane for Chromium ions removal. *IOP Conf. Ser. Earth Environ. Sci.* **2021**, *779*, 012099. [[CrossRef](#)]
29. Verma, S.; Dutta, R.K. A facile method of synthesizing ammonia modified graphene oxide for efficient removal of uranyl ions from aqueous medium. *RSC Adv* **2015**, *5*, 77192–77203. [[CrossRef](#)]
30. Song, B.; Li, L.; Lin, Z.; Wu, Z.-K.; Moon, K.-s.; Wong, C.-P. Water-dispersible graphene/polyaniline composites for flexible micro-supercapacitors with high energy densities. *Nano Energy* **2015**, *16*, 470–478. [[CrossRef](#)]
31. Pruna, A.I.; Barjola, A.; Cárcel, A.C.; Alonso, B.; Giménez, E. Effect of varying amine functionalities on CO₂ capture of carboxylated graphene oxide-based cryogels. *Nanomaterials* **2020**, *10*, 1446. [[CrossRef](#)]
32. Karimi, A.; Rajabi, M.; Zahedi, P. Effect of graphene oxide content on morphology and topography of polysulfone-based mixed matrix membrane for permeability and selectivity of carbon dioxide and methane. *Mater. Und Werkst.* **2020**, *51*, 1137–1147. [[CrossRef](#)]
33. Xia, S.; Yao, L.; Zhao, Y.; Li, N.; Zheng, Y. Preparation of graphene oxide modified polyamide thin film composite membranes with improved hydrophilicity for natural organic matter removal. *Chem. Eng. J.* **2015**, *280*, 720–727. [[CrossRef](#)]
34. Tang, L.A.; Lee, W.C.; Shi, H.; Wong, E.Y.; Sadovoy, A.; Gorelik, S.; Hogley, J.; Lim, C.T.; Loh, K.P. Highly wrinkled cross-linked graphene oxide membranes for biological and charge-storage applications. *Small* **2012**, *8*, 423–431. [[CrossRef](#)]
35. Mohseniazar, M.; Barin, M.; Zarredar, H.; Alizadeh, S.; Shanehbandi, D. Potential of microalgae and lactobacilli in biosynthesis of silver nanoparticles. *BioImpacts* **2011**, *1*, 149. [[PubMed](#)]
36. Ayyaru, S.; Ahn, Y.-H. Application of sulfonic acid group functionalized graphene oxide to improve hydrophilicity, permeability, and antifouling of PVDF nanocomposite ultrafiltration membranes. *J. Membr. Sci.* **2017**, *525*, 210–219. [[CrossRef](#)]
37. Chen, D.; Cheng, Y.; Zhou, N.; Chen, P.; Wang, Y.; Li, K.; Huo, S.; Cheng, P.; Peng, P.; Zhang, R.; et al. Photocatalytic degradation of organic pollutants using TiO₂-based photocatalysts: A review. *J. Clean. Prod.* **2020**, *268*, 121725. [[CrossRef](#)]

Disclaimer/Publisher’s Note: The statements, opinions and data contained in all publications are solely those of the individual author(s) and contributor(s) and not of MDPI and/or the editor(s). MDPI and/or the editor(s) disclaim responsibility for any injury to people or property resulting from any ideas, methods, instructions or products referred to in the content.